International Journal of Thermal Sciences 49 (2010) 1264–1276

Contents lists available at ScienceDirect

International Journal of Thermal Sciences

journal homepage: www.elsevier.com/locate/ijts

Finite time thermodynamics study and exergetic analysis of ammonia–water absorption systems

Brice Le Lostec [a,b], Jocelyn Millette [a], Nicolas Galanis [b,*]

[a] LTE, Shawinigan, QC, Canada G9N7N5
[b] Génie mécanique, Université de Sherbrooke, Sherbrooke, QC, Canada J1K2R1

ARTICLE INFO

Article history:
Received 16 July 2009
Received in revised form
1 December 2009
Accepted 14 February 2010
Available online 30 March 2010

Keywords:
Absorption machine
Finite time thermodynamics
Exergy
Optimization

ABSTRACT

This paper presents an optimization study of a single stage absorption machine operating with an ammonia–water mixture under steady state conditions. The power in the evaporator, the temperatures of the external fluids entering the four external heat exchangers as well as the effectiveness of these heat exchangers and the efficiency of the pump are assumed fixed. The results include the minimum value of the total thermal conductance UA_{tot} as well as the corresponding mean internal temperatures, overall irreversibility and exergetic efficiency for a range of values of the coefficient of performance (COP). They show the existence of three optimum values of the COP: the first minimises UA_{tot}, the second minimises the overall irreversibility and the third maximises the exergetic efficiency. They also show that these three COP values are lower than the maximum COP which corresponds to the convergence of the internal and external temperatures towards a common value. The influence of various parameters on the minimum thermal conductance of the heat exchangers and on the corresponding exergy efficiency has also been evaluated. From an exergetic viewpoint it is interesting to reduce the temperature at the desorber and at the evaporator and to raise the values of that parameter at the condenser and the absorber. However these changes must be accompanied by an important increase in the total *UA* if it is desired to conserve a constant COP. The internal heat exchangers between the working fluid and the solution improve both the overall exergy efficiency and the coefficient of performance of the absorption apparatus.

1. Introduction

Industrial energy wastes are, by definition, non- or under-utilized sources of energy which should be re-examined from the perspective of recovered energy, minimisation of adverse environmental impacts and optimization of energy use. In order to improve energy efficiency, the valorisation of such thermal energy wastes can be achieved by introducing, where appropriate, a process for cooling or air-conditioning such as the absorption machine. Some approaches have been developed to evaluate and enhance the efficiency of this energy transformation process. In particular, the coefficient of performance is used to evaluate the performance and the efficiency of such cold producing systems. This method only takes into account the first law of thermodynamics. Also, when different sources and forms of energy are involved within a system, none of the criteria of the process describes its performance from the viewpoint of the energy quality involved. This factor is taken into account by the second law of thermodynamics and appears in the exergetic analyses.

Finite time thermodynamics optimizations have already been described and applied to absorption machines. Optimizations of heat transfer surfaces, of performance coefficients and of the maximum available power have been carried out [1]. Chen [2] has studied the optimal internal temperatures of fluids and the production of entropy taking place in the energy transfer between the reservoirs and the internal cycle. The internal irreversibility of the cycle has also been presented [3–8]. A new method for the optimization of thermal systems, based on finite time thermodynamics, has been proposed by Stitou and Feidt [9]. The real irreversible cycle is compared to an ideal cycle, for which non-zero temperature differences are used to estimate the heat transfer between the cycle and the heat reservoirs. The aim of this method is to calculate the minimal heat exchanger surface and the optimal internal temperatures of an endo-irreversible cycle, taking into account the internal irreversibilities. Exergetic studies of absorption machines have also been published [10,11]. This type of

* Corresponding author. Tel.: +1 819 821 7144; fax: +1 819 821 7163.
E-mail address: nicolas.galanis@usherbrooke.ca (N. Galanis).

1290-0729/$ – see front matter © 2010 Elsevier Masson SAS. All rights reserved.
doi:10.1016/j.ijthermalsci.2010.02.005

Nomenclature

A	Heat transfer surface (m^2)
COP	Coefficient of performance
ΔT_{LM}	Log mean temperature difference (K)
e	Specific exergy (J kg^{-1})
$\Delta\dot{E}$	Rate of exergy destruction (W)
h	Specific enthalpy (J kg^{-1})
$\dot{m}$	Mass flow rate (kg s^{-1})
Q	Heat transfer rate (W)
$\dot{S}$	Entropy generation rate (W K^{-1})
s	Specific entropy (J kg^{-1} K^{-1})
T	Temperature of the external streams (K)
t	Internal temperatures of the absorption machine (K)
U	Thermal conductance (W m^{-2} K^{-1})
W	Electric power (W)
x	Non-dimensional heat transfer rate used to establish convergence

Greek letters

α	Non-dimensional heat transfer rate related to energy expenses
β	Non-dimensional heat transfer rate related to energy utilities
η	Efficiency
θ	Carnot factor ($1 - T_0/T$)
λ	Lagrange multiplier
σ	Entropy production flux with respect to energy expense (W K^{-1})
ψ	Internal irreversibility coefficient
ω	Optimization parameter (see Eq. (5))

Indices

α	Absorber
c	Condenser
cr	Combination of condenser and pre-condenser
d	Desorber
E	Exergetic
e	Evaporator
in	Inlet
int	Internal
out	Outlet
p	Pump
r	Pre-condenser
tot	Total
0	Environment surrounding the absorption machine

analysis essentially applies the 2nd law of thermodynamics to determine the destruction of exergy or the internal irreversibility of the cycle.

The combination of a thermodynamic optimization in finite times and of an exergetic analysis has not been applied to absorption machines. It is then pertinent to analyse, following the second law of thermodynamics, an absorption machine having been optimized by a finite time thermodynamic analysis method in order to identify the least efficient components. Furthermore, the finite time thermodynamic analysis of an endo-irreversible process requires the knowledge of the internal irreversibility coefficient. The latter can be calculated, rather than imposed as in the study by Stitou and Feidt [9], by simulating the performance of an absorption machine. Inter-dependence between the finite time thermodynamic optimization and the simulation of the cycle itself for the exergetic analysis is therefore obtained.

This paper presents such a study based on the finite time thermodynamics optimization coupled with the exergetic analysis of an absorption machine. The power in the evaporator, the temperatures of the external fluids entering the four external heat exchangers as well as the effectiveness of these heat exchangers and the efficiency of the pump are assumed fixed. Initially the minimum total thermal conductance of the heat exchangers and the corresponding internal temperatures of the absorption machine are calculated for different values of the coefficient of performance. In a second step, the exergy analysis for the operating conditions corresponding to minimum total thermal conductance determines the value of the coefficient of performance which optimizes the operation of the absorption machine according to the 2nd law of thermodynamics.

2. Absorption cooling

Absorption cooling machines are similar to compression refrigerating or air-conditioning machines. The major difference is that they use thermal energy (absorber – desorber) and no mechanical or electrical energy in the driving part of the cycle. The fluids used in an absorption cycle are composed of a refrigerant and of an absorbent. In the present study, ammonia is used as the refrigerant and water as the absorbent. Thus the system requires a rectification column and/or a pre-condenser (rectifier) to purify the vapour leaving the desorber as illustrated in Fig. 1.

The high pressure refrigerant liquid (2) leaving the condenser is sub-cooled in the refrigerant heat exchanger RHX. The liquid (11) is expanded (3) and then evaporated in the evaporator. The resulting vapour (4) is superheated in the RHX. It is then necessary to compress this vapour before reinjecting it into the condenser. For this purpose the superheated vapour (12) is absorbed in a weak ammonia–water mixture (5) in the absorber and then compressed by the pump from (6) to (7). The desorber and rectification column separate the ammonia from the water to complete the cycle. States 23 and 24 are the outlet and inlet to the rectification column while states 8 and 9 are the inlet and outlet to the desorber. The solution heat exchanger SHX permits an internal recovery of thermal

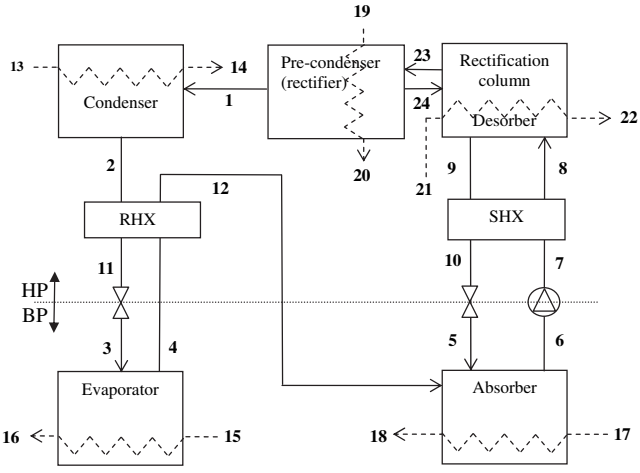

Fig. 1. Schematic representation of the system.

energy, thus lowering the evacuated energy at the absorber and the energy provided to the desorber. External streams indicated by discontinuous lines in Fig. 1 act as heat sources or sinks in the condenser, evaporator, absorber, desorber and pre-condenser.

In the present study the values of the evaporator power Q_e, the temperature of the external streams entering the corresponding five heat exchangers (T_{13}, T_{15}, T_{17}, T_{19} and T_{21}), the effectiveness of all heat exchangers and the efficiency of the pump are fixed.

3. Finite time thermodynamics

Finite time thermodynamics allow the study of thermodynamic cycles by taking into account the temperature differences between the sources or the sinks and the internal temperatures of the cycle. The purpose of this analysis is to calculate these temperature differences and the corresponding thermal conductance of the external heat exchangers. The objective is the minimisation of the total heat transfer conductance and the evaluation of the corresponding distribution among the external heat exchangers for a given coefficient of performance. In order to simplify the calculations it is assumed that the fluid leaving the rectification column at (23) and circulating through the condenser, RHX and evaporator is pure ammonia. The external stream entering the condenser is the same as that entering the pre-condenser and their temperature is identical ($T_{13} = T_{19}$). Therefore these two units are treated as a single one in the finite time thermodynamics formulation. The adopted methodology is based on the general theory developed by Stitou and Feidt [9] who assumed constant values for U as well as for the source/sink temperatures and calculated the minimum total surface of the heat exchangers for a general energy conversion system. In the present study, the summation of the UA products is minimised, rather than the surface itself, based on mean temperatures of the external streams (the expressions defining these mean temperatures in terms of the corresponding inlet temperatures are specified in Section 5). The relations and procedure used for this minimisation are presented in the next paragraphs of the present section.

By defining the following non-dimensional quantities [9]:

$$\alpha_d = \frac{Q_d}{Q_d+Q_p}, \beta_{cr} = \frac{Q_{cr}}{Q_d+Q_p}, \beta_a = \frac{Q_a}{Q_d+Q_p}, \mathrm{COP} = \frac{Q_e}{Q_d+Q_p} \tag{1a}$$

$$\sigma_{int} = \frac{S_{int}}{Q_d+Q_p}, \psi = 1+\frac{\sigma_{int}}{\frac{\alpha_d}{t_d}} \tag{1b}$$

the first law of thermodynamics (normalised by reference to energy expenditures $Q_d + Q_p$) becomes

$$\alpha_d + (1-\alpha_d) - \beta_{cr} - \beta_a + \mathrm{COP} = 0 \tag{2}$$

Analogously, the second law of thermodynamic is [9]:

$$\psi\frac{\alpha_d}{t_d} - \frac{\beta_{cr}}{t_{cr}} - \frac{\beta_a}{t_a} + \frac{\mathrm{COP}}{t_e} = 0 \tag{3}$$

By considering a transfer law of the Fourier type, the total UA is equal to:

$$UA_{tot} = \frac{Q_d}{(T_d-t_d)} - \frac{Q_{cr}}{(T_{cr}-t_{cr})} - \frac{Q_a}{(T_a-t_a)} + \frac{Q_e}{(T_e-t_e)} \tag{4}$$

Minimisation of UA_{tot} when the independent variables t_i are constrained by Eq. (3) is achieved by the Lagrange multipliers method which provides the following result [9]:

$$\frac{1}{\lambda} = \psi\left(\frac{T_d-t_d}{t_d}\right)^2 = \left(\frac{T_{cr}-t_{cr}}{t_{cr}}\right)^2 = \left(\frac{T_a-t_a}{t_a}\right)^2 = \left(\frac{T_e-t_e}{t_e}\right)^2 = \omega^2 \tag{5}$$

The internal temperatures of the absorption machine can then be calculated from Eq. (5).

$$\frac{1}{t_d} = \frac{1}{T_d}\left(1+\frac{\omega}{\sqrt{\psi}}\right) \tag{6}$$

$$\frac{1}{t_e} = \frac{1}{T_e}(1+\omega) \tag{7}$$

$$\frac{1}{t_a} = \frac{1}{T_a}(1-\omega) \tag{8}$$

$$\frac{1}{t_{cr}} = \frac{1}{T_{cr}}(1-\omega) \tag{9}$$

Replacing relations (6)–(9) into Eq. (3), which expresses the constraint for the minimisation of UA_{tot}, an expression for the optimum value of ω in terms of the external mean temperatures is obtained.

$$\omega = \frac{-\left[\psi\frac{\alpha_d}{T_d} - \frac{\beta_{cr}}{T_{cr}} - \frac{\beta_a}{T_a} + \frac{\mathrm{COP}}{T_e}\right]}{\left[\sqrt{\psi}\frac{\alpha_d}{T_d} + \frac{\beta_a}{T_a} + \frac{\beta_{cr}}{T_{cr}} + \frac{\mathrm{COP}}{T_e}\right]} \tag{10}$$

This allows the calculation of the optimum values of the internal temperatures using relations (6)–(9) and the corresponding UA_i of each thermal transfer from Eqs. (11) to (14).

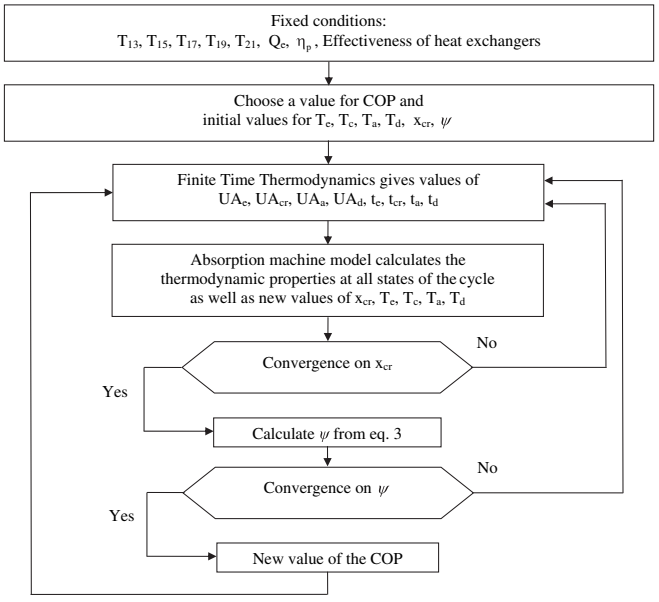

Fig. 2. Illustration of the iterative numerical solution.

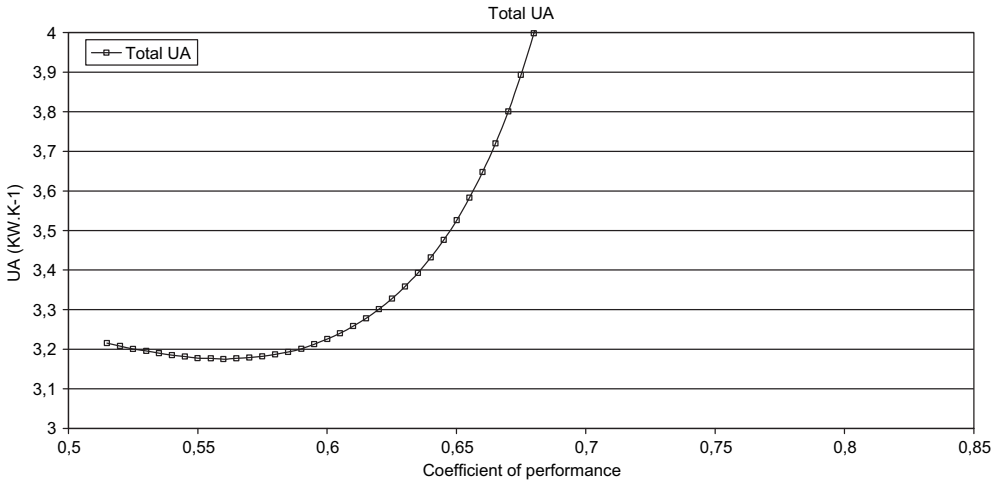

Fig. 3. Minimum total thermal conductance.

$$UA_d = (Q_d + Q_p)\frac{\alpha_d}{(T_d - t_d)} = (Q_d + Q_p)\frac{\alpha_d}{T_d}\left(1 + \frac{\sqrt{\psi}}{\omega}\right) \quad (11)$$

$$UA_e = (Q_d + Q_p)\frac{\mathrm{COP}}{(T_e - t_e)} = (Q_d + Q_p)\frac{\mathrm{COP}}{T_e}\left(1 + \frac{1}{\omega}\right) \quad (12)$$

$$UA_a = -(Q_d + Q_p)\frac{\beta_a}{(T_a - t_a)} = -(Q_d + Q_p)\frac{\beta_a}{T_a}\left(1 - \frac{1}{\omega}\right) \quad (13)$$

$$UA_{\mathrm{cr}} = -(Q_d + Q_p)\frac{\beta_{\mathrm{cr}}}{(T_{\mathrm{cr}} - t_{\mathrm{cr}})} = -(Q_d + Q_p)\frac{\beta_{\mathrm{cr}}}{T_{\mathrm{cr}}}\left(1 - \frac{1}{\omega}\right) \quad (14)$$

These equations are solved for a fixed value of Q_e and any given value of the COP by assuming initial values of the four mean external temperatures T_i (as a first approximation they are set equal to the fixed values of the corresponding temperatures at the entrance of each external heat exchanger) as well as α_d, $x_{\mathrm{cr}} \equiv \beta_{\mathrm{cr}}/(\beta_a + \beta_{\mathrm{cr}})$ and ψ (as a first approximation their initial values are set equal to 1, 0.5 and 1.1 respectively). The corresponding optimum values of the internal temperatures t_i calculated from Eqs. (6) to (9) are communicated to the model of the absorption cycle (described in Section 5) which calculates the corresponding new values of T_i, α_d and $x_{\mathrm{cr}} \equiv \beta_{\mathrm{cr}}/(\beta_a + \beta_{\mathrm{cr}})$ along with other results. The new value of ψ is then calculated from Eq. (3) and Eqs. (6) to (14) are solved once again for the updated values of the optimum internal temperatures and the individual UA corresponding to the updated minimum value of UA_{tot}. This iterative procedure, illustrated in Fig. 2, is repeated until the difference between successive values of ψ becomes less than 10^{-4}. It has been implemented using the Matlab software.

It should be noted that by virtue of Eqs. (1a) and (2) the non-dimensional ratio x_{cr} can also be expressed as

$$x_{\mathrm{cr}} = \beta_{\mathrm{cr}}/(\beta_a + \beta_{\mathrm{cr}}) = Q_{\mathrm{cr}}/(Q_{\mathrm{cr}} + Q_a) = \beta_{\mathrm{cr}}/(1 + \mathrm{COP}) \quad (15)$$

4. Exergetic analysis

The exergy balance is obtained from the energy and entropy balances that respectively correspond to the first and second laws of thermodynamics. The entropy and exergy analyses are equivalent because they permit the evaluation of the thermodynamic quality of a process. The exergy of a system represents the maximum work that can be recuperated, or that must be supplied, if it evolves towards a thermodynamic equilibrium state with the environment. In the present case, the exergy at each point in the

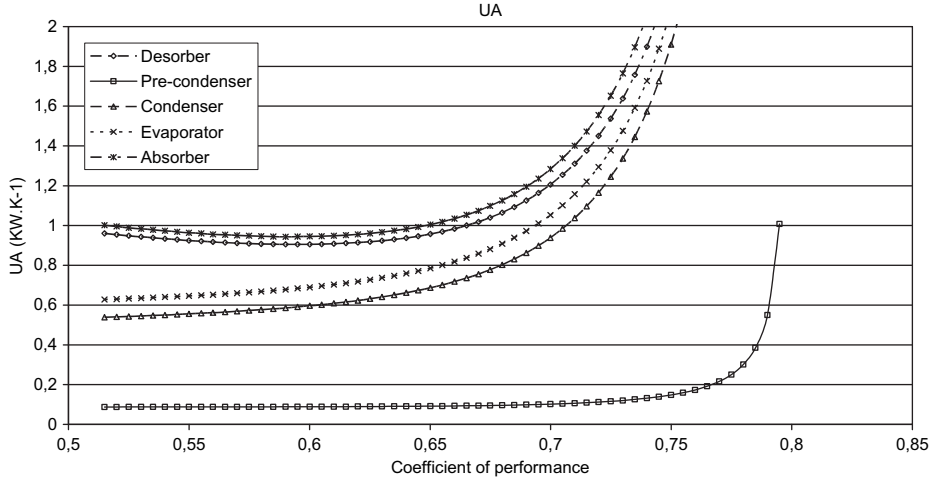

Fig. 4. Thermal conductance of each heat exchanger corresponding to the minimum UA_{tot}.

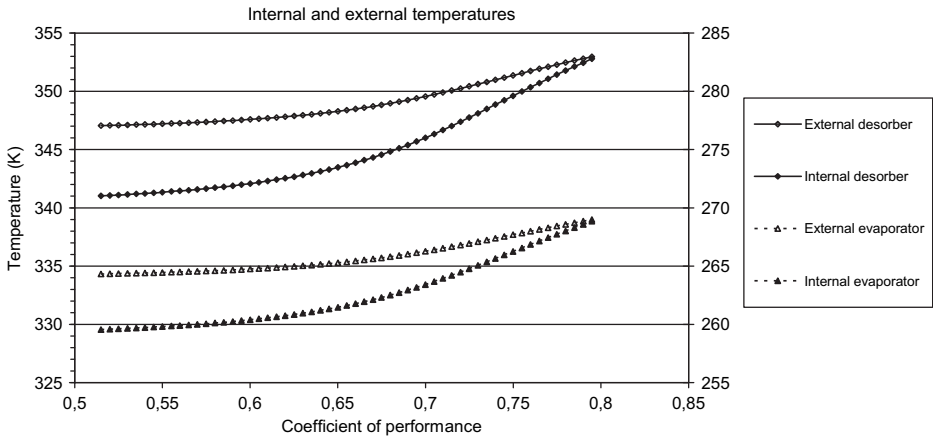

Fig. 5. Internal and external mean temperatures at the evaporator and desorber corresponding to the minimum UA_{tot}.

system is calculated from the following equation which neglects the kinetic and potential energy [12,13]:

$$e = h - h_0 - T_0(s - s_0) \tag{16}$$

The reference conditions are generally taken equal to 25 °C and 1 bar. However, if the system is in contact with more than one stream the reference temperature must be taken equal to the lowest stream temperature [14]. In the present case, this value corresponds to the temperature of the cooling water entering the condenser and the absorber. The rate of exergy destruction associated with each component of the absorption machine, without heat transfer from the surroundings, is given by the following expression [13,14]:

$$\Delta\dot{E} = \sum_{in} \dot{m}_{in} e_{in} - \sum_{out} \dot{m}_{out} e_{out} - W \tag{17}$$

The total exergy destroyed in the absorption machine is equal to the sum of the exergy destroyed in each component [10,11].

$$\Delta\dot{E}_{tot} = \sum \Delta\dot{E} \tag{18}$$

The exergetic efficiency is the ratio between the recovered exergy (at the evaporator) and the provided exergy (in the desorber) [12–14].

$$\eta_E = \frac{\dot{m}_{15}(e_{16} - e_{15})}{\dot{m}_{21}(e_{21} - e_{22})} \tag{19}$$

5. Modelling of the absorption machine

The model of the absorption machine was described in an earlier article [15]. It is based on the conservation equations for the mass, the species, the energy and on the relations proposed by Ziegler and Trepp [16] for the evaluation of thermodynamic properties of the water–ammonia mixtures. It should be noted that these values depend on three independent properties (for example the pressure, temperature and ammonia mass fraction) since the working fluid is not a pure substance. The equations by Ziegler and Trepp [16] are also reported elsewhere [17–19]. They are based on the excess Gibbs energy combined with the properties of pure fluids. The application domain is from 0.2 bar to 110 bar and from −43 °C to 327 °C for the coefficients proposed by Ibrahim and Klein [19].

The simulation of the absorption machine assumes a steady state regime and permits the calculation of the temperature, the pressure, the vapour fraction, the NH_3 concentration, the enthalpy, the entropy, the exergy and the mass flow rate at each point in the cycle. It uses the results obtained from the finite time thermodynamics optimization by equating the optimum internal temperatures calculated from Eqs. (6) to (9) with those of the working fluid

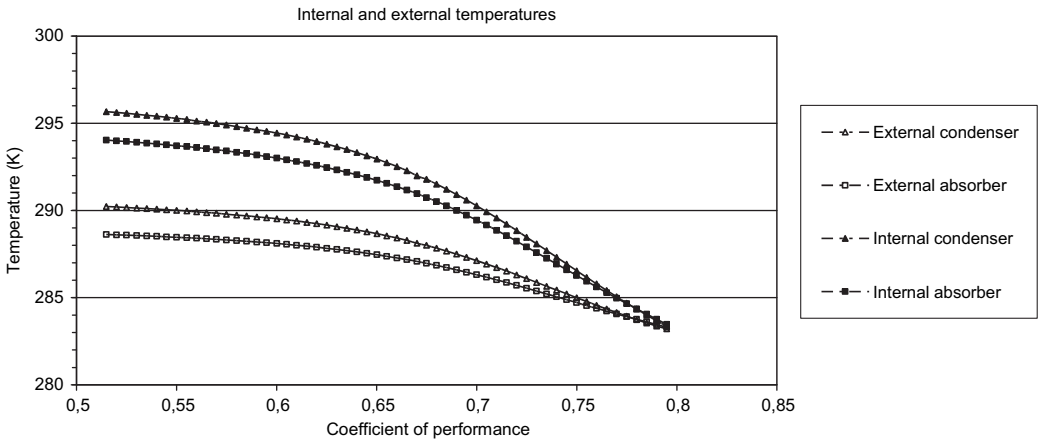

Fig. 6. Internal and external mean temperatures at the condenser and absorber corresponding to the minimum UA_{tot}.

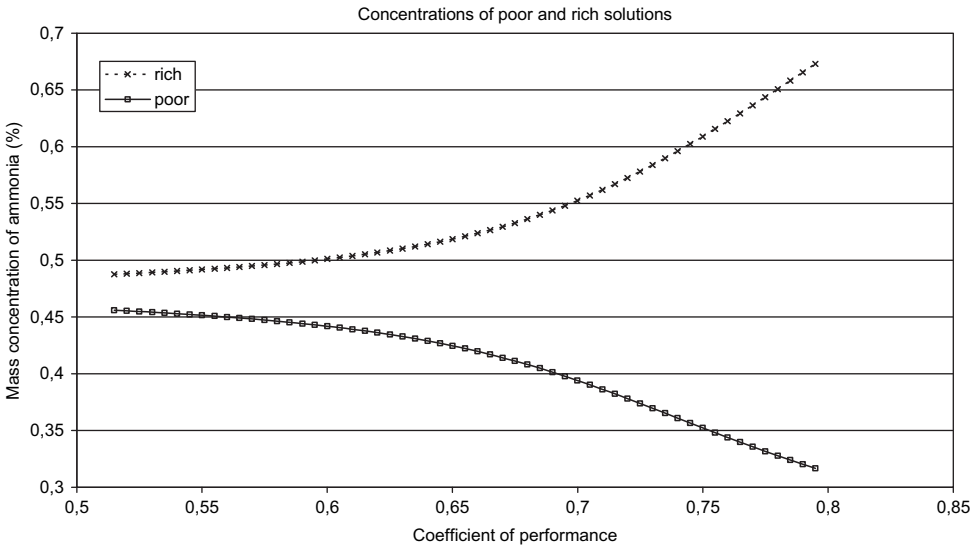

Fig. 7. Concentrations of poor and rich solutions corresponding to the minimum UA_{tot}.

at the exit from the corresponding heat exchanger in the cycle simulation. Thus, $t_{cr} = t_2$, $t_e = t_4$, $t_a = t_6$ and $t_d = t_9$. The model also incorporates the following assumptions:

- Pure ammonia in the refrigeration circuit (points 1, 2, 3, 4, 11, 12, 23 and 24 in Fig. 1)
- The external streams are an aqueous solution of ethylene glycol in the evaporator and water in the condenser, absorber, desorber and pre-condenser (The thermodynamic properties of the mixture of water–ethylene glycol are evaluated from the data in [20] and the fundamental thermodynamic equations for incompressible liquids [12] submitted to an isobaric evolution).
- Saturated liquid at the exit from the pre-condenser (24), the condenser (2), the absorber (6) and the desorber (9).
- Saturated vapour at the exit from the pre-condenser (1), the evaporator (4) and the rectification column (23)
- No pressure loss in the components
- No heat loss to the external environment

The model calculates the properties of the working fluid at every state of Fig. 1 as well as the heat transferred at each heat exchanger and the corresponding mass flow rates of the working fluid and the external fluids. The mean external temperatures T_i are then evaluated (as functions of the internal temperatures t_i) from the following equation:

$$T_i = t_i + (T_{i,out} - T_{i,in})/\ln((T_{i,out} - t_i)/(T_{i,in} - t_i)) \quad (20)$$

These updated values of the four mean external temperatures are communicated to the finite time thermodynamics optimization model which calculates a new value for ψ (see Fig. 2). The convergence is said to be satisfactory for an absolute error smaller than 0.001 for the COP and smaller than 0.002 for x_{cr}. Restrictive constraints such as a rich concentration in ammonia greater than the weak concentration and ω positive (temperatures of sources greater than the working fluid temperature and temperature of sinks lower than the working fluid temperature at the entrance of the corresponding heat exchanger) have also been imposed.

6. Results and discussions

Section 6.1 presents the results of the system optimization for the operating conditions defined in Section 5. Sections 6.2–6.5

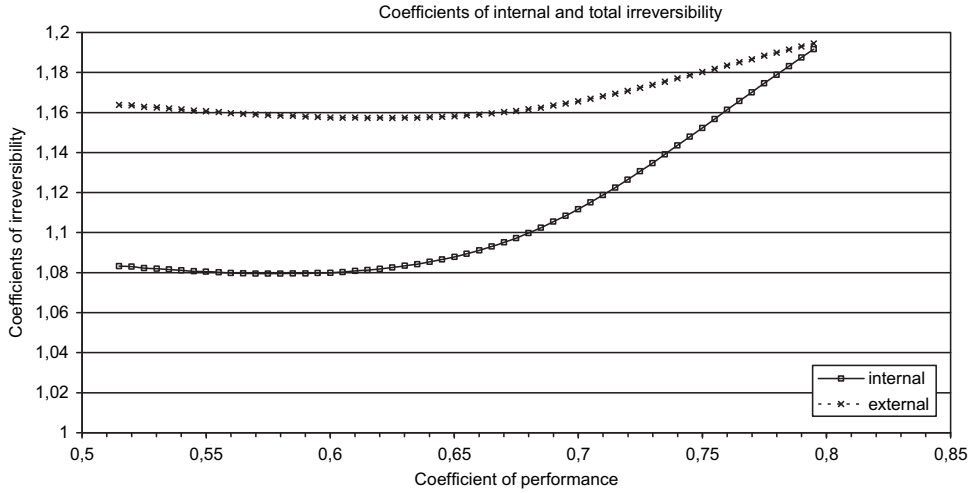

Fig. 8. Coefficients of internal and total irreversibility corresponding to the minimum UA_{tot}.

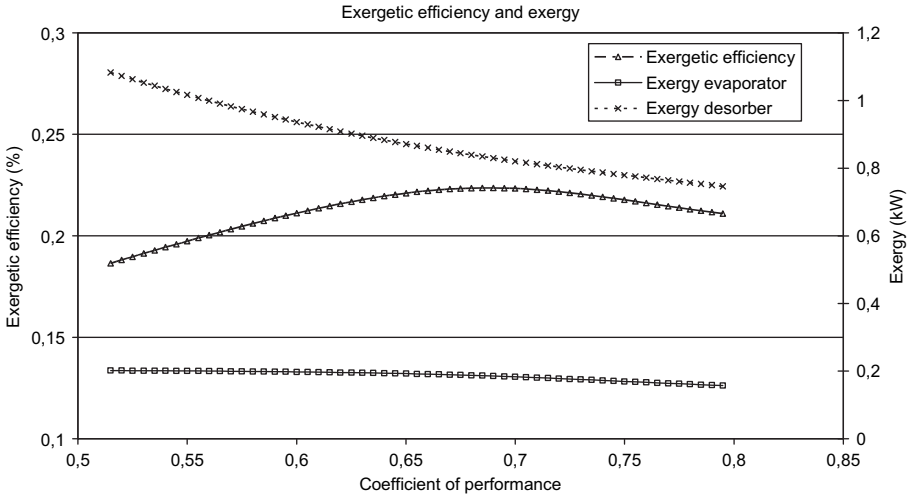

Fig. 9. Recovered exergy (evaporator), provided exergy (desorber) and exergetic efficiency corresponding to the minimum UA_{tot}.

describe the effects of varying some of the operating conditions. All these results were calculated with the iterative procedure outlined in Fig. 2 and therefore correspond to operating conditions which minimise UA_{tot}. They show the relation between the minimum value of UA_{tot} and the corresponding exergetic efficiency for different values of the COP. Thus they are a synthesis of calculations involving the first and second laws of thermodynamics as well as finite time thermodynamics and are dependant on the properties of the ammonia–water mixture whose concentration is not the same throughout the system.

The results have been obtained for the following values of the fixed parameters:

- Effectiveness of internal heat exchangers (SHX and RHX): 80%
- Effectiveness of external heat exchangers (condenser, pre-condenser, absorber, evaporator and desorber): 80% (the definition of this effectiveness and the expression of energy conservation are used to determine the mass flow rate and exit temperature of the external fluid for each of these heat exchangers)
- Isentropic efficiency of the pump: 95%
- Useful heat transfer rate (refrigeration): $Q_e = 3$ kW
- External temperature at evaporator inlet: $T_{15} = -4$ °C
- External temperature at absorber inlet: $T_{17} = 10$ °C
- External temperature at the condenser inlet: $T_{13} = 10$ °C
- External temperature at the pre-condenser inlet: $T_{19} = 10$ °C
- External temperature at the desorber inlet: $T_{21} = 80$ °C
- Reflux in the pre-condenser $\equiv \dot{m}_{24}/\dot{m}_1$: minimum reflux × 1.3 [21]
- Volumetric concentration of ethylene glycol in the external loop of the evaporator: 40% (freezing temperature: −25.3 °C)

6.1. Finite time thermodynamics and exergetic optimization

Fig. 3 shows the results of the optimization procedure described in the previous sections by presenting the minimum value of UA_{tot} as a function of the coefficient of performance. The observed relation is similar to the general results for the optimization of heat exchanger surfaces, obtained by Stitou and Feidt [9], which show

Table 1
Thermodynamic variables of the absorption system for operation at maximum exergetic efficiency.

Points	Temperature (K)	Pressure (bar)	Ammonia concentration	Enthalpy (kJ/kg)	Entropy (kJ/(kg K))	Exergy (kJ/kg)	Vapour fraction	Flow rate (kg s^{-1})
1	291.47	8.01	1.00	1280.73	4.42	274.56	1.00	0.00246
2	290.91	8.01	1.00	82.98	0.30	242.11	0.00	0.00246
3	262.94	2.99	1.00	29.20	0.13	238.74	0.06	0.00246
4	262.94	2.99	1.00	1249.38	4.75	149.69	1.00	0.00246
5	301.22	2.99	0.40	−103.43	0.29	1.02	0.00	0.00787
6	290.00	2.99	0.54	−162.22	0.09	13.82	0.00	0.01033
7	290.04	8.01	0.54	−161.55	0.09	14.43	0.00	0.01033
8	321.74	8.01	0.54	−12.14	0.58	25.72	0.00	0.01033
9	345.39	8.01	0.40	92.63	0.89	27.32	0.00	0.00787
10	301.11	8.01	0.40	−103.43	0.29	3.22	0.00	0.00787
11	279.43	8.01	1.00	29.20	0.11	241.73	0.00	0.00246
12	285.32	2.99	1.00	1303.15	4.95	147.87	1.00	0.00246
13	283.15	1.00	0.00	41.89	0.15	0.00	0.00	0.10521
14	289.81	1.00	0.00	69.88	0.25	0.32	0.00	0.10521
15	269.15	1.00	0.00	−13.58	−0.05	1.22	0.00	0.17873
16	264.18	1.00	0.00	−30.36	−0.11	2.26	0.00	0.17873
17	283.15	1.00	0.00	41.89	0.15	0.00	0.00	0.17646
18	288.63	1.00	0.00	64.93	0.23	0.22	0.00	0.17646
19	283.15	1.00	0.00	41.89	0.15	0.00	0.00	0.01207
20	289.81	1.00	0.00	69.88	0.25	0.32	0.00	0.01207
21	353.15	1.00	0.00	335.27	1.08	31.20	0.00	0.16682
22	346.94	1.00	0.00	309.25	1.00	26.23	0.00	0.16682
23	291.47	8.01	1.00	1280.73	4.42	274.56	1.00	0.00274
24	290.91	8.01	1.00	82.98	0.30	242.11	0.00	0.00028

that the *UA* tends towards infinity when the coefficient of performance approaches the irreversible maximum COP (this is the value for an endo-irreversible machine with zero temperature difference between the working fluid and the external streams). It is interesting to note in Fig. 3 the existence of an absolute minimum for UA_{tot} corresponding to a COP value approximately equal to 0.56. In Fig. 4 the corresponding *UA* values associated with each heat transfer process between the sinks or sources and the internal cycle are plotted as functions of the COP. Each of these five *UA* values tends towards infinity when the COP approaches the irreversible maximum COP. On the other hand, the *UA* of the utility (evaporator) should tend towards zero when the COP approaches 0. This cannot be seen on the curves of Fig. 4 because of the applied constraints on rich and poor concentrations. In other words, it is not possible for the system to operate under the conditions defined in the previous sections with a COP smaller than approximately 0.52.

Figs. 5 and 6 show the mean internal and external temperatures of the evaporator, the desorber, the absorber, and the condenser/pre-condenser combination for operation with the minimum UA_{tot}. When the COP rises beyond 0.6 the internal temperature for each component approaches the corresponding mean external temperature and, therefore, the *UA* value increases rapidly (cf. Fig. 4). In addition, the mean external temperature for each heat exchanger tends towards the corresponding inlet temperature or, equivalently, the temperature change of the sources and sinks tends to zero.

As the internal temperatures approach the temperature of the corresponding secondary fluid at the heat exchanger inlet and the *UA* and COP increase, the difference between the concentrations of the rich (points 6, 7, 8) and poor (points 5, 9, 10) solutions increases (Fig. 7). For these conditions, the need for vapour purification is more important because of the decrease of the poor solution concentration.

In Fig. 8, the coefficients of internal and total irreversibility are shown as functions of the COP for operation with the minimum UA_{tot}. They converge towards a common value as the COP increases towards its maximum value. This is caused by the fact that the mean internal and external temperatures approach each other when the COP increases (see Figs. 5 and 6). Therefore, the irreversibility of the heat transfer process, which corresponds to the difference between corresponding points on the two curves of Fig. 8, decreases and becomes zero when the COP reaches its maximum. It is interesting to note the existence of a minimum value for the coefficient of total irreversibility corresponding to a COP approximately equal to 0.62.

Fig. 9 shows the variations of the recovered exergy at the evaporator (numerator of Eq. (19)) and the provided exergy at the desorber (denominator of Eq. (19)) for operation with the minimum UA_{tot}. They both decrease when the COP increases for the reasons given in the previous paragraph, albeit at different rates. As a result, the exergetic efficiency (which is equal to their ratio) reaches a maximum for COP $\approx$ 0.69. When the COP increases beyond this value and the mean external temperatures tend towards the inlet temperature of the corresponding secondary fluid (see Figs. 5 and 6) the exergetic efficiency decreases.

At the conditions of maximum exergetic efficiency, the operating characteristics of the absorption machine are described in Tables 1–3. It should be noted that the properties of pure fluids (water and ammonia) are evaluated from the equations for the ammonia–water mixture. The condensation and evaporation temperatures for points 1, 2 and 23, 24 are therefore slightly different because of the difference between the condensation and boiling curves for ammonia concentrations of 0 and 1 proposed by [19]. In accordance with the previously stated assumptions, pure ammonia circulates between the exit of the desorber and the inlet of the absorber. The concentrations of the weak and rich solutions are 0.40 and 0.54 respectively while the high and low pressures in the binary cycle are 8.01 and 2.99 bar respectively. According to the results of Table 2, the exergy destruction principally takes place in the absorber and the desorber and is caused by the mixing of the fluids. The internal heat exchanger SHX (regenerator) is the cause of 13% of the exergy destruction. However, its presence lowers the exergy destruction in the absorber and in the desorber. Similar results have been obtained by [10] and [11]. Table 3 shows that at the exergetic optimum ($\eta_E = 0.22$ at COP = 0.69; cf. Fig. 9) the difference between the mean temperatures of the working fluid and the external sources or sinks is between 3 K and 4 K in each of the external heat exchangers.

Table 2
Energy fluxes and rate of exergy destruction for operation at maximum exergetic efficiency.

Component	Heat transfer (internal) (W)	Exergy destroyed (external and internal) (W)	
Evaporator	3000	−33.44	5.81%
Condenser	−2945	−45.73	7.95%
Absorber	−4066	−190.00	33.03%
Desorber	4341	−195.99	34.07%
Heat exchanger (7–8)	1544	−73.16	12.72%
Heat exchanger (9–10)	−1544		
Pump	7	−0.62	0.11%
Expansion valve (11–3)	0	−8.27	1.44%
Expansion valve (10–5)	0	−17.33	3.01%
Heat exchanger (4–12)	132	−5.41	0.94%
Heat exchanger (2–11)	−132		
Pre-condenser	−338	−5.24	0.91%
Total	0	−575.20	100.00%

Fig. 10 provides a visualisation of the exergy destruction associated with the thermal transfers between the reservoirs and the internal cycle. The Carnot factor θ, defined in conformity to [9], is expressed as follows for the external and internal temperatures respectively:

$$\theta_{T_i} = 1 - \frac{T_0}{T_i} \quad \theta_{t_i} = 1 - \frac{T_0}{t_i} \tag{22}$$

These results show that exergy destruction is more important in the absorber and the desorber. In order to reduce these contributions to the total exergy destruction the corresponding internal temperatures t_a and t_d must be as close as possible to the mean external temperatures T_a and T_d respectively. This is equally confirmed by reference to Figs. 6 and 8. To limit the unused exergy, the mean external temperature of the absorber and the condenser

Table 3
Mean temperatures and performance indicators for operation at maximum exergetic efficiency.

	Component	Temperature (K)
External	Desorber	349.25
	Condenser	287.50
	Evaporator	266.03
	Absorber	286.59
Internal	Desorber	345.39
	Condenser	290.91
	Evaporator	262.94
	Absorber	290.00
Coefficient of performance		0.69
Exergetic efficiency		0.22
Irreversibility coefficient		1.16

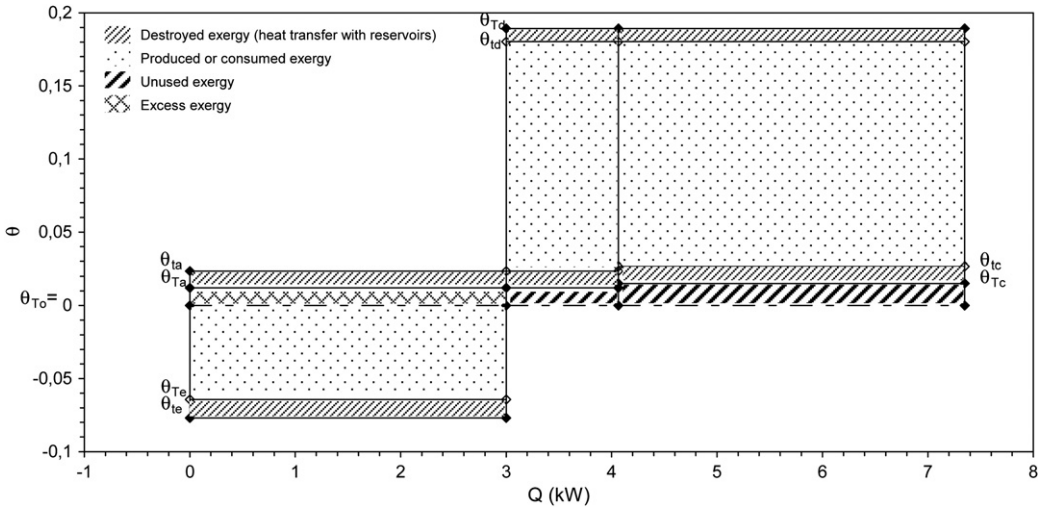

Fig. 10. $\theta = f(Q)$ diagram for the system under consideration.

should be equal to the environment temperature T_0. This would be obtained by an infinite heat exchanger surface, such as observed in Figs. 3 and 8 and is therefore not practical.

The results in this section have shown the existence of three optimums. The first corresponds to the minimisation of the UA_{tot} (Fig. 3), the second corresponds to the minimisation of the overall irreversibility (Fig. 8) and the third corresponds to the maximisation of the exergetic efficiency (Fig. 9). These optimums are obtained for COP values of 0.56, 0.62 and 0.69 respectively.

6.2. Influence of the external temperature at the desorber inlet

Fig. 11 shows that for any given value of the COP the exergetic efficiency increases when the inlet temperature to the desorber (T_{21}) decreases. These quantitative results reflect the intuitively expected tendency that, for a constant COP, the machine becomes more efficient with regard to the 2nd law when it receives energy of lower quality.

Fig. 11 also indicates that the maximum attainable COP (which corresponds to an infinite UA_{tot} as illustrated in Fig. 3) and the COP corresponding to the maximum exergetic efficiency decrease as T_{21} increases. This behaviour is attributed to two causes:

- On the one hand, the need for rectification increases since the water concentration at the desorber exit (23) increases with temperature. Therefore the reflux ($\dot{m}_{24}$) increases and the mass flow rate of ammonia through the evaporator decreases. To maintain a fixed refrigeration effect Q_e it is then necessary to increase the energy input to the desorber Q_d and therefore the COP decreases (see Eq. (1a)).
- On the other hand, the energy needed to heat the solution from T_8 to the saturation temperature increases with T_{21} since the effectiveness of the solution heat exchanger SHX is constant. This extra energy is supplied by the heat source in the desorber and appears in the denominator of the COP expression (see Eq. (1a)).

Fig. 12 shows the minimum value of UA_{tot} as a function of the COP for different values of the desorber inlet temperature T_{21}. For a fixed low value of the COP the minimum UA_{tot} decreases as T_{21} increases. However, since the maximum COP decreases as T_{21} increases while the corresponding minimum value of UA_{tot} tends towards infinity, the lines of constant T_{21} intersect. Hence, for high values of the COP the minimum UA_{tot} increases as T_{21} increases.

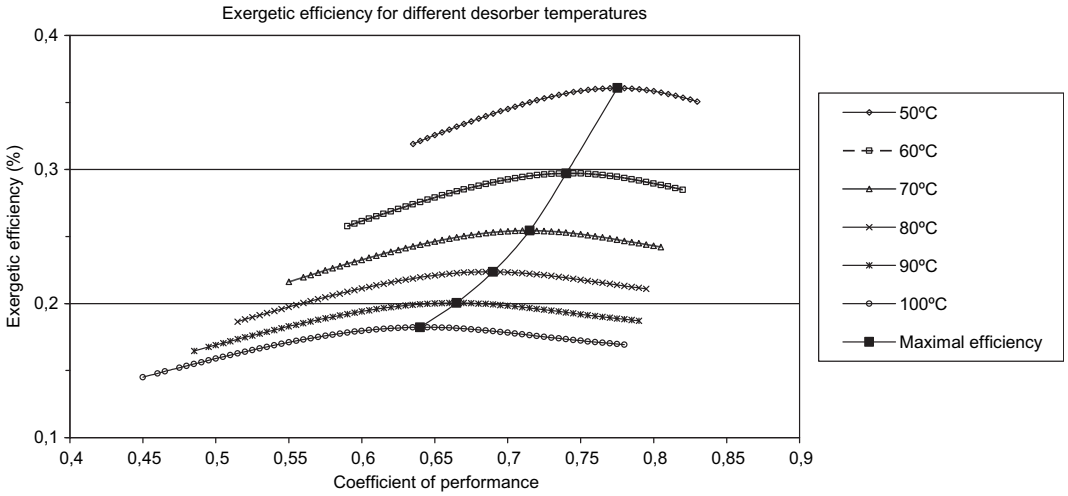

Fig. 11. Exergetic efficiency corresponding to the minimum UA_{tot} for different desorber temperatures.

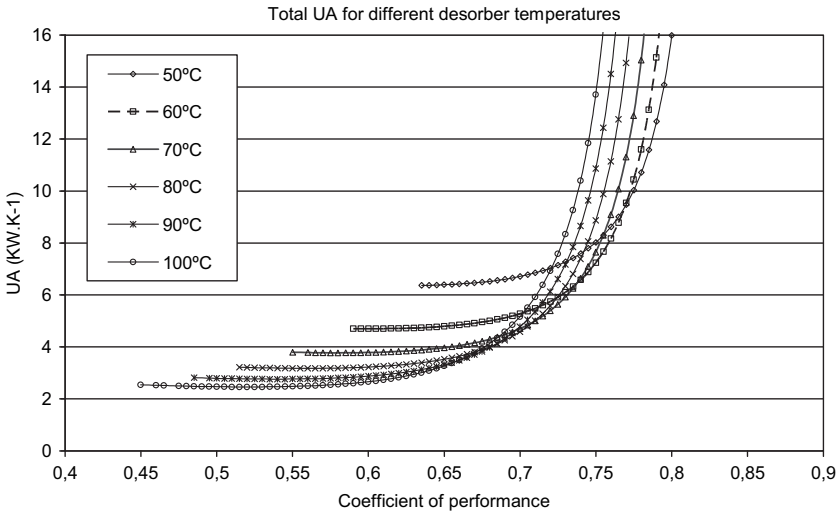

Fig. 12. Minimum UA_{tot} for different desorber temperatures.

6.3. Influence of the inlet temperature to the condenser and the absorber

Throughout this study these two temperatures (T_{13} and T_{17}) have been set equal to the same value which is also used to define the dead state for the exergy calculations (Eq. (16)). Therefore the results of Fig. 13 which show the exergetic efficiency for different values of these two temperatures are not based on the same reference state. However, the fact that η_E increases as these two temperatures increase is qualitatively understandable since, under these circumstances the quality of the energy at the evaporator increases while that of the energy at the desorber decreases.

Fig. 13 also indicates that the maximum attainable COP increases as these two temperatures decrease while the COP corresponding to maximum exergetic efficiency is not influenced much by this parameter.

Fig. 14 shows that the total thermal conductance increases significantly when the common value of these two temperatures increases. Thus, for example, for COP = 0.65 the total thermal conductance for $T_{13} = T_{17} = 16$ °C is almost double the corresponding value for $T_{13} = T_{17} = 8$ °C. These results underline the necessity for a technico-economic analysis to determine the cost associated with the heat exchangers.

6.4. Influence of the inlet temperature to the evaporator

Fig. 15 shows that the exergetic efficiency increases significantly when the inlet temperature to the evaporator (T_{15}) decreases. This is logical since the conditions of the high temperature heat source (T_{21}) and the intermediate temperature heat sinks ($T_{13} = T_{12}$) are fixed. On the other hand the maximum attainable COP decreases as T_{15} decreases while the COP for which η_E is maximum does not vary much with T_{15}.

Fig. 16 indicates that the range of economically interesting COP values (i.e. those for which the UA_{tot} is relatively low) decreases significantly as T_{15} decreases. For COP = 0.6 the minimum required thermal conductance is approximately three times higher for $T_{15} = -20$ °C than for $T_{15} = 0$ °C.

6.5. Influence of SHX and RHX exchangers

The regeneration, or internal transfer of energy, in the solution heat exchanger and the refrigerant heat exchanger lowers the internal irreversibility coefficient and increases the exergetic efficiency. Fig. 17 shows the evolution of the exergetic efficiency as a function of the COP, with or without these internal heat exchangers. The presence of the internal heat exchangers increases

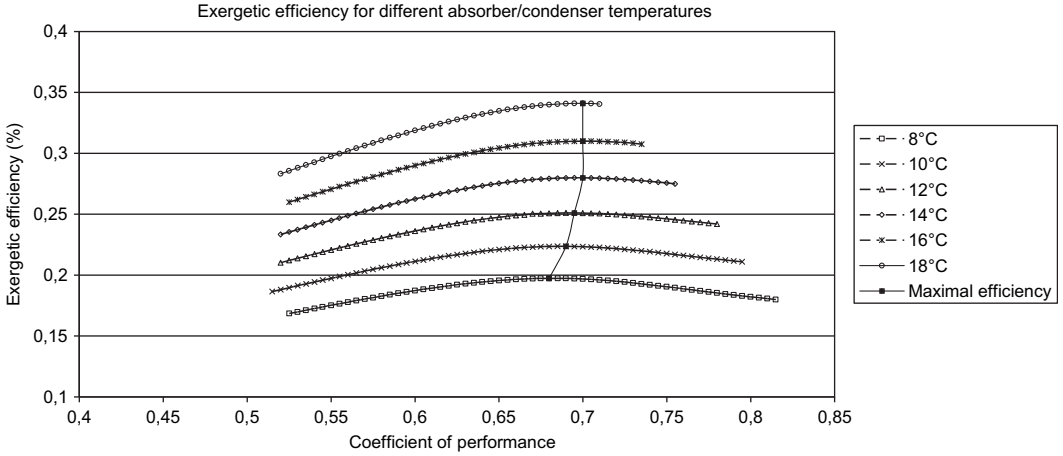

Fig. 13. Exergetic efficiency corresponding to the minimum UA_{tot} for different values of the common temperature at the inlets of the absorber and the condenser ($T_{13} = T_{17}$).

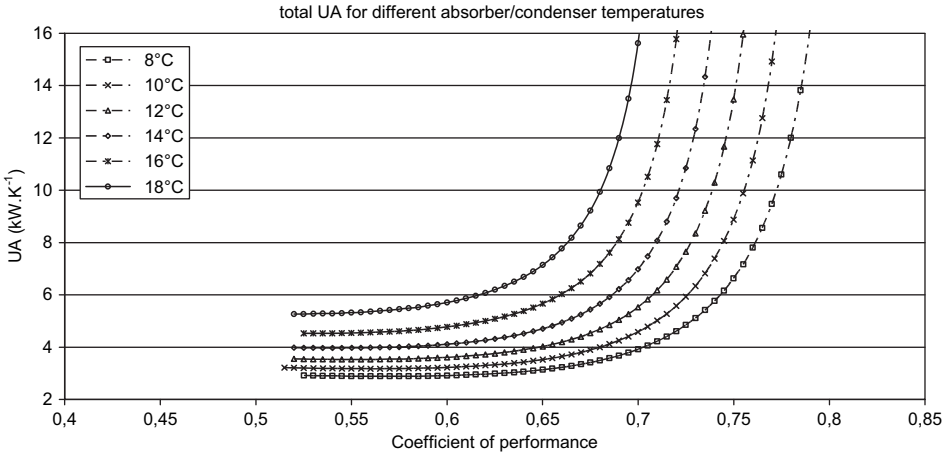

Fig. 14. Minimum UA_{tot} for different absorber/condenser inlet temperatures.

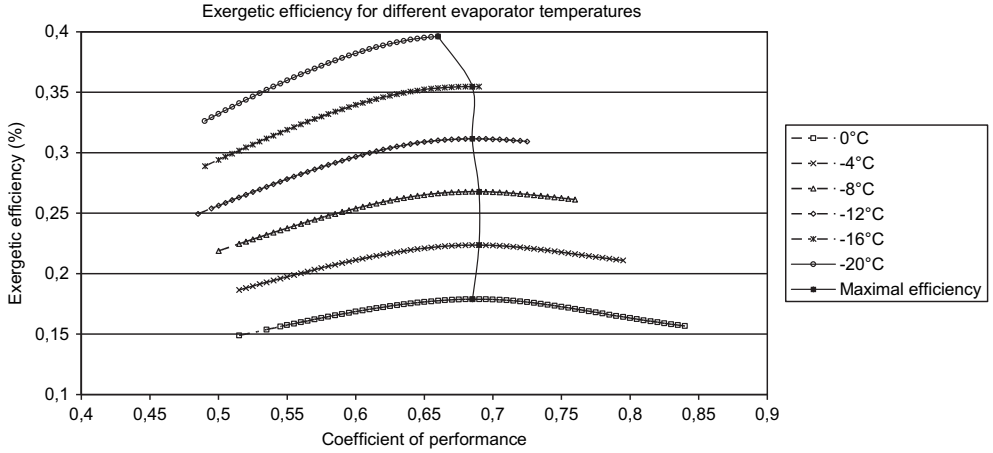

Fig. 15. Exergetic efficiency corresponding to the minimum UA_{tot} for different evaporator temperatures.

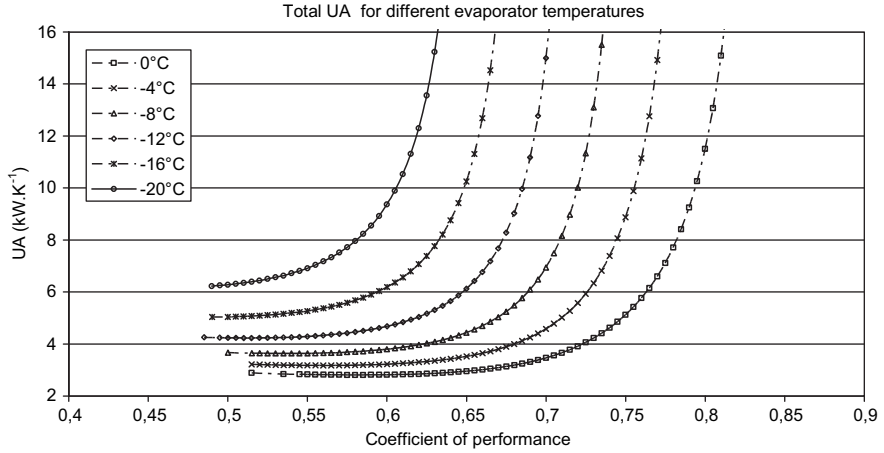

Fig. 16. Minimum UA_{tot} for different evaporator inlet temperatures.

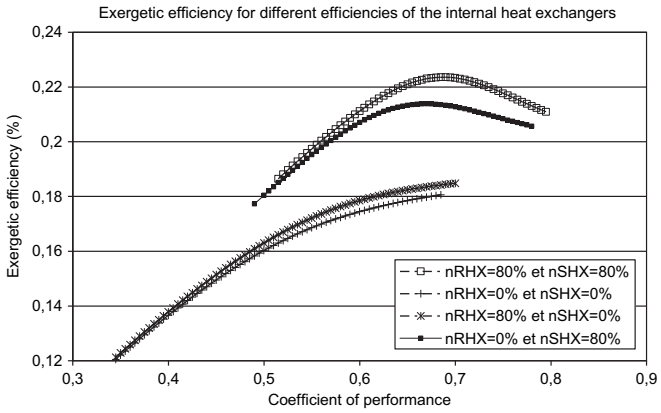

Fig. 17. Exergetic efficiency for different values of the internal heat exchangers effectiveness.

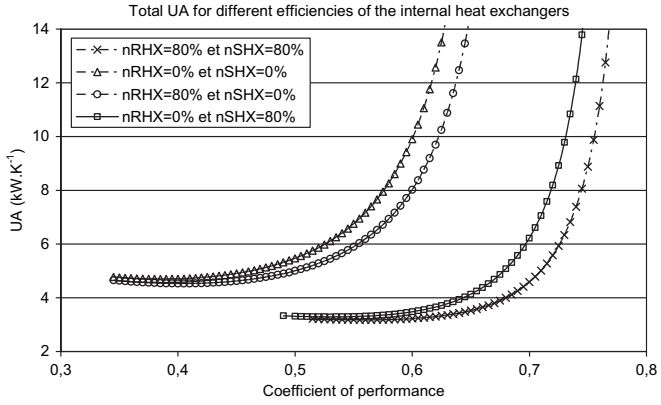

Fig. 18. Minimum UA_{tot} for different values of the internal heat exchangers effectiveness.

the maximum attainable COP and increases the exergetic efficiency of the absorption machine for a fixed COP. According to these results it is the SHX that has the greatest influence and that generates the greatest improvement between results with and without internal heat exchangers. The RHX is associated with a small energy transfer (Table 2); this can explain its small but not negligible influence on the system. Qualitatively similar results regarding the influence of these two heat exchangers on the COP of the absorption machine were presented by Heppenstall [22] who arrived at the same conclusions.

Fig. 18 presents the minimum total *UA* for heat transfer between the external reservoirs and the internal cycle as a function of the COP, with and without the SHX and RHX exchangers. These results show that, for a fixed COP, the total *UA* decreases considerably when the internal exchangers are incorporated in the cycle. Furthermore, for the same *UA*, the COP increases by 15–25% when internal heat exchangers are installed. So, before trying to improve the heat transfer between sources or sinks and the internal cycle, it is preferable to use internal heat exchangers. In fact the SHX is present in the majority of absorption machines.

7. Conclusions

A simulation tool, based on finite time thermodynamics and the first two laws of classical thermodynamics, has been developed for the purpose of predicting the performance and the operating characteristics of a single stage absorption cooler working with the ammonia–water mixture. It has led to the determination of the minimum total thermal conductance of the external heat exchangers of the system, its distribution among these heat exchangers and the corresponding internal temperatures associated with each heat transfer process for a given coefficient of performance. An exergetic analysis of this optimized system was then performed. The results show the existence of three optimum values of the coefficient of performance: the first is approximately equal to 0.56 and minimises the total *UA*, the second is approximately equal to 0.62 and minimises the overall irreversibility while the third is approximately equal to 0.69 and maximises the exergetic efficiency. The results also show that the destruction of exergy takes place mostly in the absorber and the desorber (respectively 33% and 34% of the total) due to the mixing or separation of the streams of binary fluids. High exergetic efficiencies are obtained for a coefficient of performance situated between 0.65 and 0.70, which implies a high UA_{tot}, a situation which may not be acceptable from an economic viewpoint.

In the future, it will be interesting to improve this method by taking into account pressure losses as well as the subcooling and the superheating of the working fluid where appropriate.

Acknowledgments

This project is part of the R&D program of the NSERC Chair in Industrial Energy Efficiency established in 2006 at Université de Sherbrooke. The authors acknowledge the support of the Natural Sciences & Engineering Research Council of Canada, Hydro Québec, Rio Tinto Alcan and CANMET Energy Technology Center.

References

[1] J. Chen, B. Andresen, Optimal analysis of primary performance parameters for an endoreversible absorption heat pump. Heat Recovery Systems & CHP 15 (8) (1995) 723–731.
[2] J. Chen, The equivalent cycle system of an endoreversible absorption refrigerator and its general performance characteristics. Energy 20 (10) (1995) 995–1003.
[3] P.K. Bhardwaj, S.C. Kaushik, S. Jain, Finite time optimization of an endoreversible and irreversible vapour absorption refrigeration system. Energy Conversion and Management 44 (2003) 1131–1144.
[4] T. Zheng, L. Chen, F. Sun, C. Wu, Performance optimization of an irreversible four-heat-reservoir absorption refrigerator. Applied Energy 76 (2003) 391–414.
[5] T. Zheng, L. Chen, F. Sun, C. Wu, The influence of heat resistance and heat leak on the performance of a four-heat-reservoir absorption refrigerator with heat transfer law of $Q \propto \Delta(T^{-1})$. International Journal of Thermal Sciences 43 (2004) 1187–1195.
[6] P.K. Bhardwaj, S.C. Kaushik, S. Jain, General performance characteristic of an irreversible vapour absorption refrigeration system using finite time thermodynamic approach. International Journal of Thermal Sciences 44 (2) (2005) 189–196.
[7] L. Chen, X. Qin, F. Sun, C. Wu, Irreversible absorption heat-pump and it's optimal performance. Applied Energy 81 (1) (2005) 55–71.
[8] L. Chen, T. Zheng, F. Sun, C. Wu, Irreversible four-temperature-level absorption refrigerator. Solar Energy 80 (2006) 347–360.
[9] D. Stitou, M. Feidt, Nouveaux critères pour l'optimisation et la caractérisation des procédés thermiques de conversion énergétique. International Journal of Thermal Sciences 44 (12) (2005) 1142–1153.
[10] A. Şencan, K.A. Yakut, S.A. Kalogirou, Exergy analysis of lithium bromide/water absorption systems. Renewable Energy 30 (5) (2005) 645–657.
[11] M.M. Talbi, B. Agnew, Exergy analysis: an absorption refrigerator using lithium bromide and water as working fluids. Applied Thermal Engineering 20 (7) (2000) 619–630.
[12] M.J. Moran, H.N. Shapiro, Fundamentals of Engineering Thermodynamics, fifth ed. John Wiley & Sons Inc, 2006.
[13] U.A. Çengel, M.A. Boles, Thermodynamics an Engineering Approach, fifth ed. McGraw-Hill, 2005.
[14] A. Bejan, G. Tsatsaronis, M. Moran, Thermal Design and Optimization. John Wiley & Sons Inc, 1996.
[15] B. Le Lostec, N. Galanis, J. Baribeault, J. Millette, Wood chip drying with an absorption heat pump. Energy 33 (3) (2008) 500–512.
[16] F. Ziegler, C. Trepp, Equation of state for ammonia–water mixtures. International Journal of Refrigeration 7 (2) (1984) 101–106.

[17] F. Yu, Y. Goswami, Thermodynamic properties of ammonia–water mixtures for power-cycle applications. Energy 24 (6) (1999) 525–536.
[18] E. Thorin, C. Dejfors, G. Svedberg, Thermodynamic properties of ammonia–water mixtures for power-cycle. International Journal of Thermophysics 19 (2) (1998) 501–509.
[19] O.M. Ibrahim, S.A. Klein, Thermodynamic properties of ammonia–water mixtures. ASHRAE Transactions 99 (1) (1993) 1495–1502.
[20] ASHRAE, 2001, 2001 ASHRAE handbook Fundamentals. Physical Properties of Secondary Coolants (Chapter 21).
[21] J.P. Moulin, D. Pareau, M. Rakip, M. Stambouli, A. Isambert, Transfert de matière Distillation compartimentée idéale, Techniques de l'ingénieur J1072.
[22] T. Heppenstall, Absorption cycle heat pumps. Heat Recovery Systems 3 (2) (1983) 115–128.